

An X-ray view of Pictor A radio lobes: a spatially resolved study

G. Migliori^{1,2,3}, P. Grandi², G.C.G. Palumbo¹, G. Brunetti⁴,
C. Stanghellini⁴

¹*Dipartimento di Astronomia, Università di Bologna, via Ranzani 1, 40127 Bologna, Italy*

²*Istituto di Astrofisica e Fisica Cosmica-Bologna, INAF, Via Gobetti 101, I-40129 Bologna, Italy*

³*SISSA/ISAS, Via Beirut 2-4, I-34014, Trieste, Italy*

⁴*Istituto di Radioastronomia-Bologna, INAF, Via Gobetti 101, I-40129 Bologna, Italy*

Abstract. A spatially resolved analysis of the lobes of the radio galaxy Pictor A has been performed for the first time starting from a 50 ksec XMM-Newton observation. Magnetic field, B_{IC} , particle density, particle to magnetic field energy density ratios have been measured. Our study shows that B_{IC} varies through the lobes. On the contrary, a rather uniform distribution of the particles is observed. In both the lobes, the equipartition magnetic field, B_{eq} , is bigger than the Inverse Compton value, B_{IC} , calculated from the radio to X-ray flux ratio.

1. Introduction

The X-ray observatories *Chandra* and *XMM-Newton* have made possible focusing on the X-ray extended emission from the faintest X-ray components of a radio galaxy, the lobes. The first aim has been to define the origin of the X-ray emission: thermal, due to external gas, compressed by the expansion of the lobes (Kraft et al. 2000; Reynolds et al. 2001), or non-thermal, due to Inverse Compton (IC) by relativistic electrons with $\gamma \sim 10^3$ on CMB photons (Harris & Grindlay 1979; Miley 1980). In the last case, we can use X-ray fluxes together with radio fluxes to obtain a direct estimate of the average magnetic field (B_{IC}) along the line of sight and, independently, the number densities of the IC emitting particles in the lobes. This method has allowed to go beyond and, at the same time, to check the validity of the classical assumption of the minimum energy condition (equipartition) in the extended regions. Even though the subject is still highly debated (Hardcastle et al. 2002; Isobe et al. 2002; Grandi et al. 2003; Croston et al. 2005), however it seems reasonable to conclude that the equipartition argument represents a viable zero-order reference guide. Also the study of the variations of the magnetic field and particle densities turns out to be useful to acquire informations on the dynamical plasma evolution in the lobes. Even though this procedure has been applied only to a few radio galaxies because of observational limits, the results indicate an enhancement of the magnetic energy density towards the edge of the lobes (Tashiro et al. 2001; Isobe et al. 2002,

2005).

2. Pictor A

Here we present a study of the lobes of the radio galaxy Pictor A, based on a new *XMM-Newton* observation of 50 ksec. The origin of the X-ray emission was exhaustively discussed in some previous papers (Grandi et al. 2003; Hardcastle & Croston 2005), and in Migliori et al. (2006) we reported the preliminary spectral analysis from this last 50 ksec observation, conducted on two datasets accumulated on the east and west lobe regions (respectively E and W regions hereafter). The extended X-ray emission is confirmed to be due to non-thermal processes, i.e. IC on CMB photons (for a detailed discussion see Migliori et al. (2007), Fig. 1 and Tab. 1 for a recap of the spectral analysis). The originality of the work on this new observation rather resides in the possibility of realize a spatially resolved study of the lobes, investigating the possible variations of the physical conditions inside the lobes themselves. For this reason we accumulated EPIC/MOS1 data sets from selected rectangular regions, three for each lobe, labeled as described in Fig. 1. Since the low number of counts, we obtained X-ray fluxes, $F_{0.5-2 \text{ keV}}$, for each subregion, once fixed the X-ray spectral slope, Γ , referring to the value, $\Gamma = 1.8$, found for the spectra of the E and W regions.

3. Discussion

Combining the X-ray fluxes at 1 keV, $F_{1 \text{ keV}}$, with the correspondent radio fluxes, $F_{1.4 \text{ GHz}}$, derived at 20 cm from the VLA image produced by Perley et al. (1997), the magnetic field B_{IC} can be immediately estimated from the formula:

$$B_{IC} = \left[\frac{F_{1.4 \text{ GHz}} C_{IC}(\alpha)(1+z)^{\alpha+3}}{F_{1 \text{ keV}} C_{syn}(\alpha)} \right]^{\frac{1}{\alpha+1}} \left[\frac{\nu_{syn}}{\nu_{IC}} \right]^{\frac{\alpha}{\alpha+1}}. \quad (1)$$

where C_{IC} and C_{syn} are quantities depending only from $\alpha = \Gamma - 1 = \alpha_x = \alpha_R$, with α_x and α_R X-ray and radio spectral indices, and $V = A \times s$ is the volume, A being the area (arcsec²) projected on the sky plane and s the thickness of the analyzed region. From synchrotron radio and Compton scattered X-ray luminosities (see Blumenthal & Gould 1970), also the other physical quantities, i.e. the electron density, k_e , magnetic field and particle energy densities, respectively u_m and u_{e+p} , are calculated. The results are reported in Tab. 2 together with the values found for the E and W regions, corresponding to the average physical conditions in the two lobes.

The two lobes (E and W regions) show very similar physical conditions, both for the magnetic field ($B_{IC} \sim 3 \mu G$) and the particle density k_e . In particular, from the ratio $u_{e+p}/u_m \sim 50 \pm 10$, it emerges that the energetic of the lobes appears to be dominated by the particles, hinting at a possible departure from the equipartition principle. Using the equipartition formula revised by Brunetti et al. (1997), we calculated the equipartition magnetic fields, B_{eq} , for both the two lobes. We found that B_{eq} overestimates B_{IC} by a factor of ~ 3 .

The equipartition estimate depends on some poorly known physical parameters such as the minimum energy of the relativistic electrons and the proton to electron energy ratio. However in Migliori et al. (2007) we have shown that our conclusion are not changed even by allowing these parameters to vary within a viable physical range. Interesting results derive from the spatially resolved analysis in spite of quite large uncertainties. In fact, if no change in the electron density appears evident in the different subregions of the two lobes, on the other side, Tab. 2 gives an indication that B_{IC} increases behind the east hot spot (e2 region in Fig. 1) where the radio flux is higher. A variation of the magnetic field was also considered in the model proposed by Hardcastle & Croston (2005). When the data from both lobes are combined together, the previous results are strengthened. Plotting B_{IC} and k_e as a function of the radio flux (divided for the corresponding sub-region volume), like in Fig. 2, we find a statistically significant variation of B_{IC} ($\chi^2 = 4.7$ with a probability $p = 3.0 \times 10^{-4}$). A *Spearman test* gives a correlation coefficient $r = 0.8$ with a $s = 0.0499$ significance: B_{IC} seems to trace the variation of the radio flux density. Once again, this behaviour is not reflected in the k_e trend (Fig 2, *Upper panel*), and the correlation test gives $r = 0.31$ with $s = 0.54$.

The possibility of variation of the spectrum of emitting electrons through the lobes is a critical issue as these variations may force B_{IC} - radio trends. Anyway, an analysis of the spectral index radio maps between 20 and 6 cm and between 6 and 2 cm (kindly provided by R. Perley and shown in Fig. 5 of Perley et al. 1997) shows negligible spectral index variations ($\Delta\alpha \leq 0.05$) from a sub-region to another one, confirming the robustness of our result.

The resulting picture might indicate a dynamical decoupling between the magnetic field and the electron energy densities as found in 3C452 by Isobe et al. (2002, 2005). A possibility is that plasma and high energy electrons expand on different scales: the first in the regions immediately beyond the hot spots, while the second on larger scales giving a fairly constant density distribution. This is in line with the picture, of a decreasing magnetic field with the increasing distance from the hot spots, proposed by Blundell & Rawlings (2000) to explain the discrepancy between the radiative lifetimes of electrons and dynamical ages of double radio galaxies. The presence of a spatial gradient of the magnetic field was also suggested by Wiita & Gopal-Krishna (1990) to justify the lack of spectral aging in the case of the lobes of 3C 234.

Acknowledgments. We are very grateful to R. Perley for kindly providing quantitatively analyzable radio images of Pictor A.

References

- Blumenthal, G. R., Gould, R. J., 1970, *RvMP*, 42, 237
- Blundell, K. M., & Rawlings, S., 2000, *AJ*, 119, 1111
- Croston, J. H., et al., 2005, *ApJ*, 626, 733
- Brunetti, G., et al., 1997, *A&A*, 325, 898
- Grandi, P., et al., 2003, *ApJ*, 586, 123
- Hardcastle, M. J., et al., 2002, *ApJ*, 581, 948
- Hardcastle, M. J., Croston, J. H., 2005, *MNRAS*, 363, 649
- Harris, D. E., & Grindlay, J. E., 1979, *MNRAS* 188, 25
- Isobe, N., et al., 2002, *ApJ*, 580, L111

- Isobe, N., et al., 2005, ApJ, 632, 781
 Kraft, R. P., et al., 2000, ApJ, 531L, 9
 Migliori, G., et al., 2006, ESASP 604, 645
 Migliori, G., et al., 2007, ApJ accepted (arXiv:0704.2131)
 Miley, G., 1980, ARA&A 18, 165M
 Perley, R. A., et al., 1997 A&A 328, 12
 Reynolds, C. S., Sebastian, H., Begelman, M. C., 2001, ApJ, 549L, 179
 Tashiro, M., et al., 2001, ApJ, 546, L19T
 Wiita, J. P., & Gopal-Krishna, 1990, ApJ, 353, 476

Figure 1. (On the left)-XMM-Newton/MOS1 image (0.2-10 keV) of Pictor A observed on January 2005. The blue and the red circles (respectively on the left and on the right respect to the nuclear region) represent the east (E) and west (W) extraction regions of the lobes used for the spectral analysis. The nucleus, two hot spots, jet contribution and a point source (black circles) are excluded. (On the right)-VLA map (Perley et al. 1997) at 20 cm. Rectangular (pink) boxes represent the subregions used for the spatially resolved analysis: e1, e2, e3 for the east lobe, w1, w2, w3, for the west lobe. Again, black circle delimitates the excluded nuclear region.

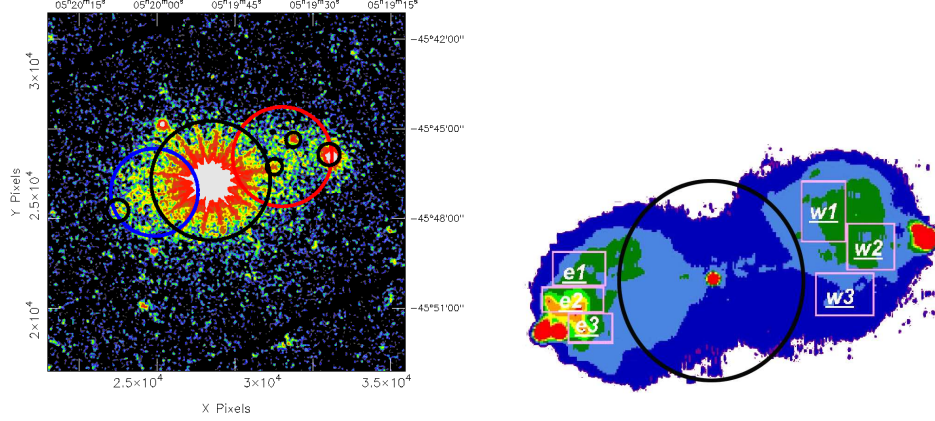


Table 1. XMM-Newton fit to the Western, W, and Eastern, E, Lobe of Pictor A in the 0.5-10 keV band. Two model are tested: a thermal emission from hot diffuse gas and a non-thermal radiation modeled with a pure power law. N_H is fixed to the galactic value $N_H^{Gal} = 4.18 \times 10^{20} \text{ cm}^{-2}$. The results strongly suggest a non-thermal origin of the radiation (see Migliori et al. 2007).

	PowerLaw			Thermal Emission		
	Γ	$\chi^2(dof)$	$F_{0.5-2 \text{ keV}}$ ($\text{erg cm}^{-2} \text{ s}^{-1}$)	kT (keV)	$\chi^2(dof)$	$F_{0.5-2 \text{ keV}}$ ($\text{erg cm}^{-2} \text{ s}^{-1}$)
W	$1.7_{-0.2}^{+0.2}$	29(38)	$12 \pm 1 \times 10^{-14}$	6_{-1}^{+3}	39(38)	$12 \pm 1 \times 10^{-14}$
E	$1.8_{-0.2}^{+0.2}$	33(31)	$9 \pm 1 \times 10^{-14}$	5_{-2}^{+3}	45(31)	$8 \pm 1 \times 10^{-14}$

Table 2. Magnetic field and particle energy densities of the Western, W, and Eastern, E, Lobe and spatially resolved analysis results.

	$F_{1.4GHz}$ (Jy)	$F_{0.5-2 keV}$ ($erg cm^{-2} s^{-1}$)	Area ($arcsec^2$)	B_{IC} (μG)	k_e ($\times 10^{-5} cm^{-3}$)	u_{e+p}/u_m
East lobe						
E	11.4 ± 0.3	$9.0 \pm 1.0 \times 10^{-14}$	12776 ± 383	3.1 ± 0.2	8.2 ± 1.0	56 ± 10
e1	2.5 ± 0.1	$1.9 \pm 0.3 \times 10^{-14}$	2992 ± 90	3.3 ± 0.3	7.3 ± 1.0	44 ± 11
e2	2.8 ± 0.1	$1.2 \pm 0.2 \times 10^{-14}$	1824 ± 55	4.4 ± 0.5	7.5 ± 1.6	25 ± 8
e3	2.5 ± 0.1	$1.5 \pm 0.2 \times 10^{-14}$	1872 ± 56	3.5 ± 0.3	10.2 ± 1.6	55 ± 12
West lobe						
W	13.7 ± 0.4	$12.0 \pm 1.0 \times 10^{-14}$	21408 ± 642	2.9 ± 0.2	6.5 ± 0.8	50 ± 10
w1	3.3 ± 0.1	$2.4 \pm 0.3 \times 10^{-14}$	3640 ± 109	3.2 ± 0.3	8.0 ± 1.4	51 ± 13
w2	2.8 ± 0.1	$2.4 \pm 0.3 \times 10^{-14}$	3024 ± 91	3.2 ± 0.3	8.1 ± 1.4	52 ± 13
w3	1.5 ± 0.1	$2.9 \pm 0.5 \times 10^{-14}$	3400 ± 102	2.5 ± 0.2	7.7 ± 1.1	81 ± 17

 Figure 2. B_{IC} (Lower Panel) and k_e (Upper Panel) values of east and west sub-regions are plotted as a function of the radio flux (F/V) at 1.4 GHz, normalized by the relative volume.
